

Influence of excitation waveform and oscillator geometry on the resonant pull-in of capacitive MEMS oscillators

Jérôme Juillard, Grégory Arndt, Julien Arcamone, Eric Colinet

► **To cite this version:**

Jérôme Juillard, Grégory Arndt, Julien Arcamone, Eric Colinet. Influence of excitation waveform and oscillator geometry on the resonant pull-in of capacitive MEMS oscillators. DTIP 2013, Apr 2013, Barcelona, Spain. pp.2-5. hal-00830533

HAL Id: hal-00830533

<https://hal-supelec.archives-ouvertes.fr/hal-00830533>

Submitted on 5 Jun 2013

HAL is a multi-disciplinary open access archive for the deposit and dissemination of scientific research documents, whether they are published or not. The documents may come from teaching and research institutions in France or abroad, or from public or private research centers.

L'archive ouverte pluridisciplinaire **HAL**, est destinée au dépôt et à la diffusion de documents scientifiques de niveau recherche, publiés ou non, émanant des établissements d'enseignement et de recherche français ou étrangers, des laboratoires publics ou privés.

Influence of excitation waveform and oscillator geometry on the resonant pull-in of capacitive MEMS oscillators

Jérôme Juillard
SUPELEC – E3S
Gif-sur-Yvette, FRANCE
jerome.juillard@supelec.fr

Grégory Arndt
Texas Instruments Norway AS
Oslo, NORWAY
g-arndt@ti.com

Julien Arcamone
CEA-LETI – MINATEC
Grenoble, FRANCE
julien.arcamone@cea.fr

Eric Colinet
SUPELEC – E3S
Gif-sur-Yvette, FRANCE
colinet@apix-technology.com

Abstract—The purpose of this paper is to provide a simple framework for determining the resonant pull-in of MEMS oscillators, either parallel-plate, CC-beam or cantilever, under one-sided and two-sided sinusoidal, square-wave or pulse-actuation. Furthermore, the values of the resonant and static pull-in amplitudes are calculated and tabulated, in all the considered cases.

Keywords—electrostatic actuation, resonant pull-in, MEMS design, nonlinear oscillators

I. INTRODUCTION

While static pull-in of capacitive MEMS structures is a well-known phenomenon [1], resonant pull-in, either under closed-loop (i.e. “oscillators”) or open-loop (i.e. “resonators”) capacitive actuation, has received considerably less attention [2-5]. Yet, it is of interest to determine at what amplitude a MEMS structure may oscillate without incurring instability, since this limit defines the maximal signal magnitude achievable with the MEMS structure and, hence, the effort that must be put in the design of the electronics (amplification / feedback) associated with the structure and in the MEMS/electronics interconnection scheme. As a rule, the larger the signal magnitude, the more the design constraints on the electronics and the interconnection scheme can be relaxed [6]. For example, in [2], it is shown that a parallel-plate oscillator with two-sided square-wave actuation (Fig. 1) cannot have stable oscillations with an amplitude larger than $g/\sqrt{3}$, where g is the electrostatic gap. In [7], we show that a CC-beam oscillator with two-sided pulse actuation (Fig. 1) is stable provided the amplitude is smaller than $g\sqrt{1-\delta^{2/3}}$, where $\delta = V_b^2/V_{pi}^2$ is the square of the ratio of the bias voltage V_b and the static pull-in voltage V_{pi} , defined as the value of the voltage making the central position unstable (Fig. 2). Note that in [2], the resonant pull-in amplitude is established under the hypothesis that $\delta \ll 1$.

The purpose of this paper is to provide a simple framework for determining the resonant pull-in of MEMS oscillators, either parallel-plate, CC-beam or cantilever (Fig. 1), under two-sided sinusoidal, square-wave or pulse-actuation (Fig. 3). Furthermore, the values of the pull-in amplitudes are calculated, for the 9 considered cases, for values of δ between 0 (very small bias voltage) and 1.

II. STATIC PULL-IN CALCULATION

For the three structures of Fig. 1, it is assumed that $w(x,t) = a(t)w_0(x)$, where $w_0(x)$ is the first bending mode and a is the position of the midpoint of the beam in the CC case or of its free extremity in the cantilever case,

normalized with respect to the gap ($a=1$ means that the structure touches the lower electrode). For a flat structure, $w_0(x)=1$. We derive the governing equations as in [7]. Using the Galerkin procedure leads to:

$$\ddot{a} + \frac{\dot{a}}{Q} + a = \delta(f_b(a) + v(t)f_c(a)) \quad (1)$$

where $\delta = V_b^2 / V_{pi}^2$, $V_{pi} \approx \sqrt{2kG^3 / (\epsilon_0 S)}$, k is the (modal) stiffness of the structure, S is the surface of the electrodes and $v = V_c / V_b \ll 1$. The electrostatic force consists of two terms, one corresponding to biasing:

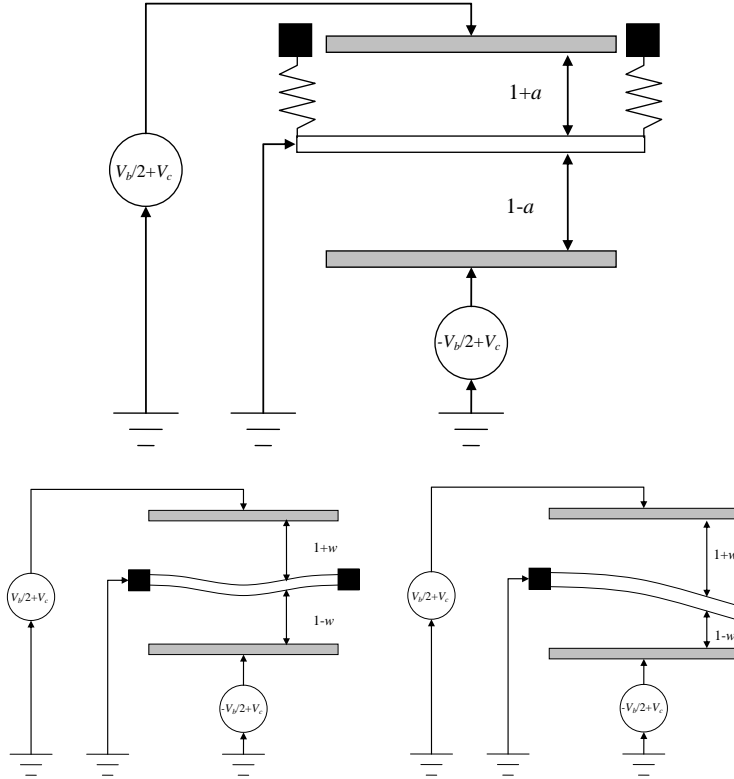


Figure 1. Parallel-plate (top), CC-beam (bottom left) and cantilever (bottom right) MEMS structures with two-sided actuation. The displacement is capacitively sensed through the middle (moving) electrode (e.g. via a charge amplifier). The upper (resp. lower) electrode is at a voltage of $V_b / 2 + V_c$ (resp. $-V_b / 2 + V_c$), where V_c is a control voltage.

$$f_b(a) = \frac{1}{4I_2} (N_{w_0}^1(2, a) - N_{w_0}^1(2, -a)),$$

the other to forcing:

$$f_c(a) = \frac{1}{I_2} (N_{w_0}^1(2, a) + N_{w_0}^1(2, -a)),$$

where, following [8], we have

$$N_{w_0}^1(2, a) = \int_0^1 w_0 (1 - aw_0)^{-2} dx$$

$$\approx \begin{cases} \frac{1}{(1-a)^2}, & \text{for a flat structure} \\ 0.523 \frac{1 + 1.74 \times 10^{-2} a}{(1-a)^{3/2}}, & \text{for a CC-beam} \\ 0.392 \left(\frac{(0.531 + 0.114a) \log(1-a)}{1-a} \right), & \text{for a cantilever} \end{cases}, \quad (2)$$

and

$$I_2 = \int_0^1 w_0^2 dx \approx \begin{cases} 1, & \text{for a flat structure} \\ 0.396, & \text{for a CC-beam} \\ 0.25, & \text{for a cantilever} \end{cases}.$$

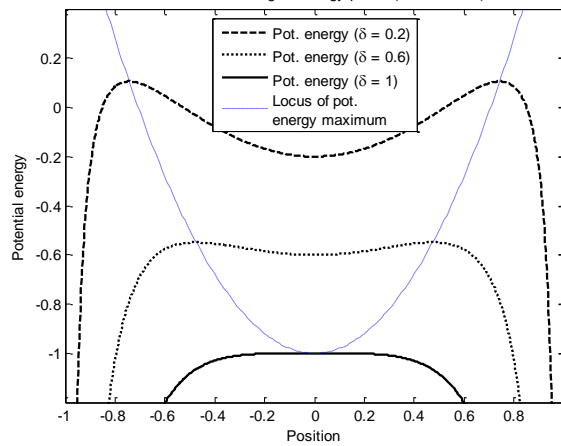


Figure 2. Potential energy (arbitrary units) vs. normalized position for a parallel-plate structure. For values of $\delta < 1$, the central position is stable and there exist two symmetric statically unstable equilibrium positions. For $\delta \geq 1$, the central position is the only equilibrium position and it is unstable.

For all three structures, the central position $a = 0$ becomes statically unstable when $\delta \geq 1$ (Fig. 2). When the central position is stable, the structures are statically pulled-in when

$$a = \delta f_b(a), \quad a \neq 0. \quad (3)$$

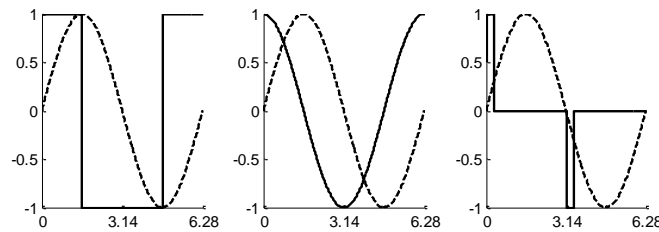


Figure 3. From left to right: square, sinusoidal and pulse waveforms (continuous line). The dashed line represents $\sin(t)$.

Using (1) and (2), one obtains $a_{pi} = \pm\sqrt{1-\delta^{1/2}}$ for a flat structure, and $a_{pi} \approx \pm\sqrt{1-\delta^{2/3}}$ for a CC-beam. In the cantilever case, the static pull-in amplitude can be approximated by $a_{pi} \approx \pm\sqrt{1-\delta^{0.9}}$.

III. RESONANT PULL-IN CALCULATION

In the absence of a DC component to the electrostatic force acting on the structure, we may assume that $a(t) = A \sin(\omega t)$. Describing function analysis [9] can then be used to study the three different actuation strategies $v(t) = v_0 \phi(t)$, where the waveform $\phi(t)$ is either a square wave, in phase with the structure velocity, a sine wave, also in phase with the structure velocity, or a ‘‘pulse wave’’, where the structure is actuated with pulses of duration τ_p (small compared to the period of the oscillation), of the same sign as \dot{a} (Fig. 3). We are interested in finding for what oscillation amplitude the structure reaches resonant pull-in in each of these three cases.

The amplitude A_{osc} and the frequency ω_{osc} of the oscillation regime corresponding to a value of v_0 are obtained by solving the nonlinear system given by the Barkhausen conditions:

$$\begin{cases} R(A, \omega) = (1 - \omega^2) - \delta J_b(A, \omega) = 0 \\ I(A, \omega) = \frac{\omega}{Q} - \delta v_0 J_c(A, \omega) = 0 \end{cases} \quad (4)$$

where

$$J_b(A, \omega) = \frac{\omega}{A\pi} \int_0^{2\pi/\omega} \sin(\omega t) f_b(A \sin(\omega t)) dt$$

and

$$J_c(A, \omega) = \frac{\omega}{A\pi} \int_0^{2\pi/\omega} \cos(\omega t) \phi(t) f_c(A \sin(\omega t)) dt.$$

The oscillation regime becomes unstable when, for $A = A_{osc}$ and $\omega = \omega_{osc}$:

$$\frac{\partial R}{\partial A} \frac{\partial I}{\partial \omega} - \frac{\partial R}{\partial \omega} \frac{\partial I}{\partial A} = 0. \quad (5)$$

In the case of square wave or sine wave excitation, J_b and J_c are independent of ω . Using (3), it is then straightforward to show that (5) is equivalent to:

$$2 \frac{J_c'}{J_c} + \delta \left(J_b' - 2 J_b \frac{J_c'}{J_c} \right) = 0, \quad (6)$$

where the prime denotes derivation with respect to A . This equation boils down to a polynomial in A in the case of a parallel-plate structure or a CC-beam. In all the considered cases, it is simple to solve it numerically. Functions J_b and J_c and their derivatives may be approximated following [8], which greatly lightens the computational load. It is notable that the resonant pull-in amplitude derived from (6) depends on the value of δ , not on that of v_0 or Q .

The case of pulse actuation is covered in [7]. It is possible to show that the resonant pull-in condition predicted by (5) corresponds to $\omega_{osc} = 0$, which is outside the range of validity of describing function analysis, and that the resonant pull-in amplitude is in fact equal to the static pull-in amplitude, predicted by (3).

The resonant pull-in amplitudes predicted by (3) – in the case of pulse-actuation – and (6) – in the case of square or sine wave actuation – are represented in Fig. 4, for the three geometries under study. We note that, in the limit of small δ , for a square-wave actuated parallel-plate structure, the same result as in [2] is found. The main result is that, for a given value of δ , the resonant pull-in amplitude is larger for a pulse-actuated

structure than for a sine-wave-actuated structure, and larger for a sine-wave-actuated structure than for a square-wave-actuated structure. In other words, the more the energy used for actuating the MEMS is concentrated in time, the more stable the oscillation is. Finally, we note that, for a given type of actuation and a given value of δ , the resonant pull-in amplitude is larger for a cantilever beam than for a CC-beam, and larger for a CC-beam than for a parallel-plate structure.

IV. DISCUSSION

Provided $Q \gg 1$, the values of the resonant pull-in amplitudes given in Fig. 4 correspond almost perfectly to those obtained through transient simulation of (1). For lower quality factor values (typically $Q < 10$), the harmonics generated by the various nonlinearities (electrostatic nonlinearity and/or actuation nonlinearity) can no longer be neglected and our predictions become less accurate. It should also be noted that, in the case of parallel-plate and CC-beam structures, the stress-stiffening (Duffing) phenomenon might also be taken into account [7]. Equation (1) would then become:

$$\ddot{a} + \frac{\dot{a}}{Q} + a(1 + \gamma a^2) = \delta(f_b(a) + v(t)f_c(a)). \quad (7)$$

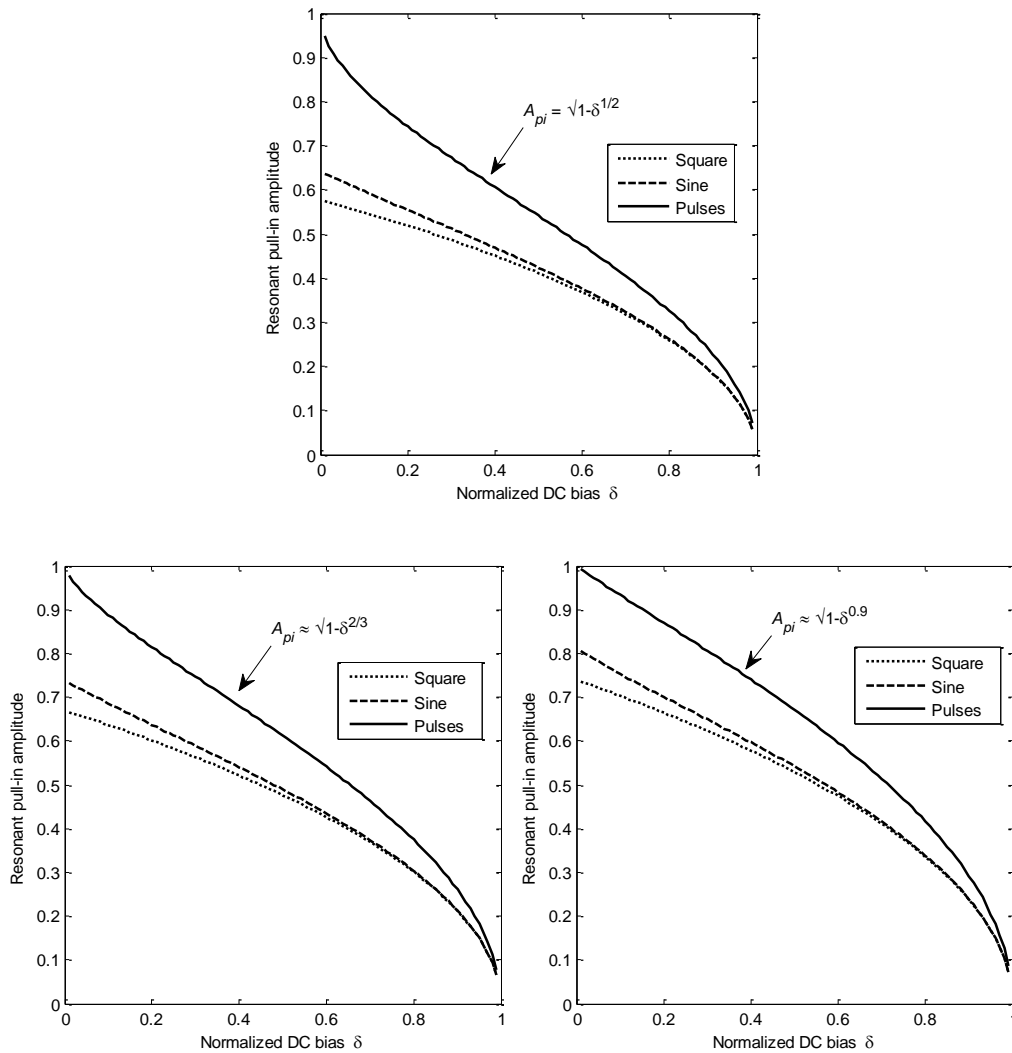


Figure 4. Normalized resonant pull-in amplitude for a parallel-plate structure (top), a CC-beam (bottom left) and a cantilever beam (bottom right). The values are obtained from (6) in the case of square-wave and sine-wave actuation or from (3) in the case of pulse-actuation

However, the approach presented in this paper can also be applied to that case. The main difference will be that the resonant pull-in amplitude will not only depend on δ , but also on the Duffing coefficient γ .

Interaction between different oscillation modes (as described in [10]) is another phenomenon limiting the validity of this study.

V. CONCLUSION

In this paper, we have shown how the resonant pull-in amplitude of different MEMS oscillators with two-sided actuation may be derived. We have shown that this pull-in amplitude depends not only on the geometry of the considered device, but also on the waveform being used for the actuation, our main result being that the more concentrated in time the actuation is, the more stable the oscillation is. The extension of this work to more complex cases (one-sided actuation, Duffing, multiple-mode interaction) is the subject of on-going work.

REFERENCES

- [1] R.C. Batra, M Porfiri, D Spinello, "Review of modeling electrostatically actuated microelectromechanical systems", *Smart Materials and Structures*, vol. 16, pp. R23-31, 2007
- [2] A. Fargas-Marques, J. Casals-Terre, A.M. Shkel., "Resonant pull-in condition in parallel-plate electrostatic actuators", *Journal of Microelectromechanical Systems*, vol. 16, pp. 1044–1053, 2007
- [3] S. Krylov, "Lyapunov exponents as a criterion for the dynamic pull-in instability of electrostatically actuated microstructures", *International Journal of Non-Linear Mechanics*, vol. 42, pp. 626 – 642, 2007
- [4] V. Leus, D. Elata, "On the dynamic response of electrostatic MEMS switches", *Journal of Microelectromechanical Systems*, vol. 17, pp. 236-243, 2008
- [5] D. Elata, H. Bamberger, "On the dynamic pull-in of electrostatic actuators with multiple degrees of freedom and multiple voltage sources", *Journal of Microelectromechanical Systems*, vol. 15, pp. 131-140, 2006
- [6] G. Arndt, "System architecture and circuit design for micro and nanoresonators-based mass sensing arrays", Ph. D. thesis, SUPELEC, 2011
- [7] J. Juillard, E. Avignon, A. Bonnoit, S. Hentz, E. Colinet, "Large amplitude dynamics of micro/nanomechanical resonators actuated with electrostatic pulses", *Journal of Applied Physics*, vol. 107, 10 pages, 2010
- [8] J. Juillard, G. Arndt, E. Colinet, "Modeling of micromachined beams subject to nonlinear restoring or damping forces", *Journal of Microelectromechanical Systems*, vol. 20, pp. 165-177, 2011
- [9] A. Gelb, W. Van der Velde, "Multiple-input describing functions and nonlinear system design", McGraw-Hill, New-York, 1968.
- [10] C. Van der Avoort et al., "Amplitude saturation of MEMS resonators explained by autoparametric resonance", *Journal of Micromechanics and Microengineering*, vol. 20, 15 pages, 2010